PHASE TRANSFORMATION AND HEAT TREATMENT

Critical Review

PHASE TRANSFORMATION AND HEAT TREATMENT IN Ti ALLOYS

Yotaro Murakami*, Department of Metallurgical Engineering, Kansai University, Suita, Osaka, 564 JAPAN (* Speaker)

Osamu Izumi, Research Institute for Iron, Steel and other Metals, Tohoku University, Sendai

Takashi Nishimura, Central Research Laboratory, Kobe Steel Ltd., Kobe

Introduction

Although much progress in the research and development of Ti alloys has been accomplished until the last Conference(1), some important works still remain to be done. Formerly the phase transformation has been studied mainly through transmission electron microscopy and X-ray diffraction techniques, which are still very useful. However, in the present time more precise techniques, for instance, high resolution electron microscopy or electron energy loss spectroscopy, have been developed to perform microanalysis of interface phase or very small precipitate such as ω phase.

The paper will review on the recent developments in the phase transformation and heat treatments in Ti alloys. This is devided into three parts entitled (i) $\alpha + \beta$ alloys, (ii) metastable β alloys, and (iii) intermetallic compounds of Ti_3Al and TiAl for high temperature use, and TiNi compound alloy with shape memory effects.

$\alpha+\beta$ alloys

The $\alpha + \beta$ alloys still dominate the use of high strength and heat resisting titanium alloys. A common practice in the treatment of $\alpha + \beta$ alloys consists of quenching or air-cooling from a high solution treatment temperature, mainly in the range of $\alpha + \beta$, and ageing subsequently at lower temperature for strengthening.

A heat treatment of quenching or air-cooling after solution treatment in $\alpha + \beta$ field, produces equiaxied α and, retained or partially transformed β phase containing hexagonal α' or orthorhombic α'' martensites(2,3). The two types of martensite decompose to $\alpha + \beta$ or $\alpha +$ (intermetallic compoud) by the subsequent low temperature ageing. The retained metastable β decomposes by phase separation (4) into two bcc phases $\beta + \beta'$ of different compositions, or by forming isothermal ω phase(5) in the β phase, or by precipitating an intermetallic compound such as an α_2 phase (6). Then, the equilibrium α phase can form either from the β' or ω phase or directly (7) from the metastable β phase.

The behavior of α'' martensite is now being noticed with keen interest in $\alpha + \beta$ alloys, because the specific changes in

yield strength, Young's modulus, and internal friction can be discussed from an intimate relationship with α" martensite. This phase is also relating to high damping property and shape memory effects, which is useful for the development of practical alloys.

The two martensites can be formed depending upon the solution treatment conditions. It was proposed that the transition in martensitic crystallography from hexagonal α' to orthorhombic α" occurs with increasing content of β stabilizing element and decreasing M_S temperatures. In this connection, it has been shown that increased α" content in a Ti-6Al-4V alloy can result from the β phase which contain 7 to 13 % V element, and notably near 10% V, and in addition the volume fraction of α" martensite tends to increase with increasing quenching rates (8). Fig. 1 shows X-ray diffraction profiles of the specimens quenched from each temperature between 1,000° and 750°C in the commercial near α-type alloy Ti-8Al-1Mo-1V(9).

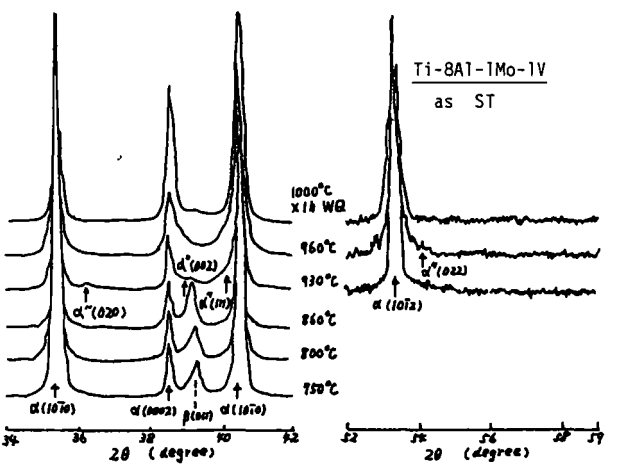

Fig. 1 : X-ray diffraction profiles of the specimens quenched from each temperature between 1,000° and 750°C in Ti-8Al-1Mo-1V

In the figure, the characteristic four (though not five) peaks of α" martensite are observed in the specimens quenched from either 900° or 960°C solution temperatures. It was also confirmed from metallographic examination that β→α" transformation was accompanied by β → α' one in the same temperature range, whereas in the higher temperature range, where the concentration of V stabilizer decreased below the level of 7 %, only α' martensite was detected to exsist. On the contrary, in β-rich α + β alloys, α" transfromation can become dominant over, and to suppress α' martensite formation. For instance, in Ti-6Al-2Sn-4Zr-6Mo alloy, it was recognized from X-ray diffraction profiles that α" transformation occurs clearly by

by quenching from the temperature above 900°C and even from the higher temperature than β- transus of 960°C, where any characteristics for α' hexagonal martensite was no longer observed from both X-ray diffraction and metallographic data. This may be due to the appropriate concentration level of Mo stabilizing element. The concentration of 6% Mo in Ti-6Al-2Sn-4Zr-6Mo alloy corresponds to the higher Mo content than about 7% level in Ti-6Al-4V alloy, which may be necessary to promote α" transformation. This is because of the fact that β - stabil-

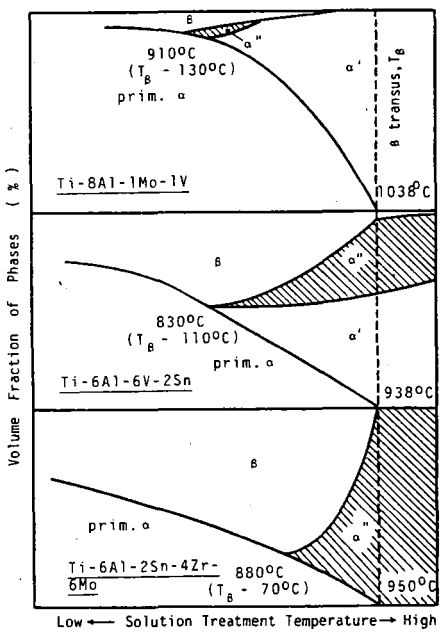

Fig. 2 : Phase transformation diagram for the three commercial alloys

zing potential of Mo is known to be one and three quarters times as much as a V - stabilizing power. The phase transformation diagram that summerise the X-ray diffraction and metallographic surveys for the three commercial alloys, Ti-8Al-1Mo-1V, Ti-6Al-6V-2Sn and Ti-6Al-2Sn-4Zr-6Mo, are shown in Fig. 2 (9). It should be noted that the α" transformation regions tend to shift towards beta transus temperatures with increasing content of β stabilizing elements, and therefore the volume fraction of α" phase is increased.

Fig. 3 shows the variation in some properties in relation to the solution treatment temperatures in Ti-6Al-2Sn-4Zr-6Mo alloy (10). From the temperature dependence of electical resistivity as shown in (a), the " martensite transformation

is clearly confirmed to occur when quenched from the solution temperature higher than about 880°C. This is in fairly good accordance with the result shown in Fig. 2. The specific values of " lowest " Young's modulus, " highest " internal friction, and " lowest " hardness shown in Fig. 3 (a), (b),and (c), respectively, can be explained in terms of an existence of α" martensite.

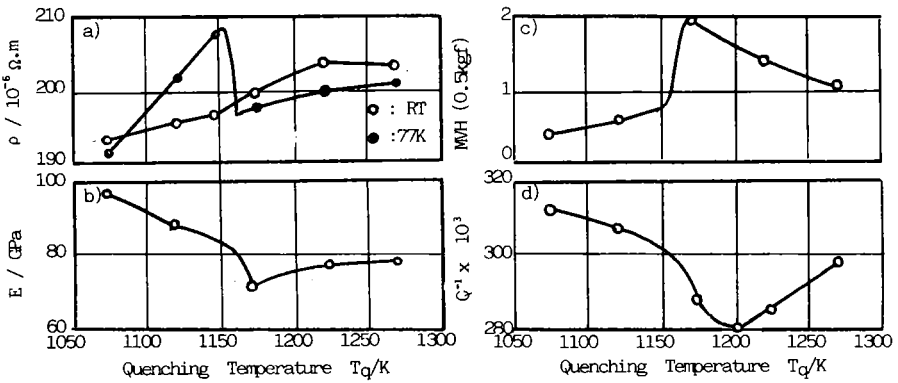

Fig. 3 : The variation in electrical resistivity (a), Young-'s modulus (b), internal friction (c), and hardness (d) in relation to the solution treatment temperatures in Ti-6Al-2Sn-4Zr-6Mo alloy (by courtecy of Sugimoto et al.)

Ito et al. have investigated the relation between the α" volume fraction and the damping capacity under the high cycle vibration in Ti-6Al-4V alloy and its base alloys, and found that an addition of 2.5 wt% Mo, which was very effective to increase the volume fraction of α" martensite, improved the damping capacity fairly well (11).

The " interface phase " is known as the microstructural features which occur under certain conditions at the interface boundaries of α and β phases. The α / β boundaries may give an important factor in fracture of two-phase Ti alloys in the case of tensile and fatigue testing, because the presence of an interfacial phase could influence the fracture process by providing an easy crack path or crack initiation sites.

Two models have been proposed for the formation of an interface phase mainly by means of transmission electron microscopy, one is a nucleation and growth mechanism by Rhodes and Paton (12), and the other a twin relationship between the interface and the alpha phase proposed by Margolin et al.(13). Up to this time, these features have been mostly examined by TEM, but it has come to be possible in the present to verify quantitatively concentration gradients by, for instance,energy-dispersive analysis employing a high resolution STEM with a resolution of about 20 nm.

Recently, Mahajan et al. (14) have examined quantitatively concentration gradients developed near the interface in the slowly cooled specimens of a Ti-6Al-2Sn-4Zr-6Mo alloy by energy-dispersive analysis as shown in Fig. 4. According to the fact

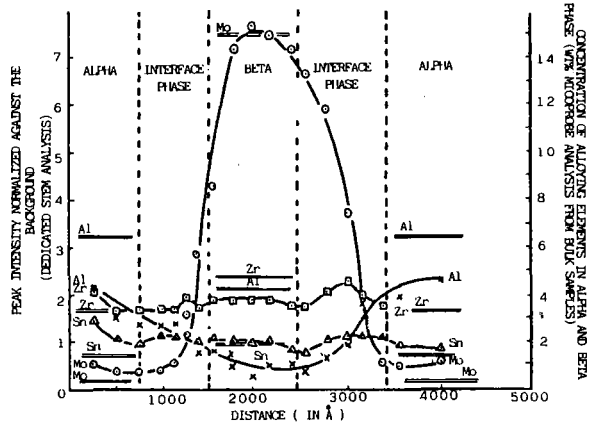

Fig. 4 : Measurements of concentration gradients of alloying elements in alpha and beta, and the interface phase by " dedicated " STEM analysis. (by courtecy of Mahajan et al.)

that a shear modulus C' is closely related to the electron concentration, these values of the β -transformed structure in this alloy were calculated from the above values of the average concentration. The electron concentration of 4.14, which was obtained at the center of β platelet is high enough to keep the phase stable, while in the interface zone, where concentration gradients vary from 4.14 at mid β platelet to 3.88 at mid α platelet, each having its C' value vanish at a different temprature during cooling process. This fact facilitates the relaxation of the volume misfit stress by the formation of the interface phase as a shear induced transformation phenomenon. This model is an extension of that proposed by Margolin et al. by using the same alloy as above, thus overturning the nucleation and growth mechanism observed in Ti-6Al-4V alloy. Further study will be necessary to understand the mechanism more clearly, by means of the precise techniques.

The new understanding of " processing-microstructure-property relations " is now being sought to improve performance specifications of high technology components. Recent advances in the development of a scientific basis for deformation processing have provided a new perspective on the traditional study of microstructure-property relationships (15).

For an α+β Ti alloy such as Ti-6Al-2Sn-4Zr-2Mo, two preform microstructures are most common. A microstructure equiaxid α phase in a matrix of transformed β phase is provided by hot working and subsequent heat treatment below the β transus temperature. This microstructure is termed " α + β ", and is known to posess good high temperature fatigue properties. On the other hand, heat treatment above β transus results, upon cooling, in a Widmanstätten α microstructure, which is termed " transformed β ", and known to have good high temperature creep properties.

Semiatin et al. have been established through compression testing and heat treatment the detailed relationships between thermomechanical processing parameters and resulting microstructures for Ti-6Al-2Sn-4Zr-2Mo-0.1Si alloy, and the following conclusions have been drawn (15).

1. Heat treatment of the α+β microstructure material below the transus temperature leads to minimal changes in the percent globular α and transformed β matrix morphology except at temperatures very near the transus. Subtransus deformation or deformation plus heat treatment lead to a significantly greater variation in the amount of primary, globular α. This finding emphasizes the improvement in transformation kinetics brought about by hot deformation or residual hot work.

2. Subtransus heat treatment of transformed β microstructure material also leads to minimal microstructural changes. Because deformed microstructures exhbit kinked platelet, it must be concluded that the general platelet morphlogy after heat treatment (and prior to deformation) remains relatively unchanged.

3. For subtransus ($T_{transus}$= 982°C) deformation of the β microstructure,for deformation at a strain of $10^{-2}s^{-1}$, the transition between these is at T ≈930°C increasing to T ≈970°C at a stain rate of 10 s^{-1}. For the low temperature regime, deformation is highy nonuniform resulting in regions of intense localized shear and bands in which the widmanstätten colonies break up and spheroidize. During post-deformation heat treatment near 954°C these regions statically recrystallize to form the equilibrium α + β microstructure. Strains greater than ε = 1, probably near ε = 5, are required for complete transformation to obtain a uniform microstracture. For deformation in the high temperature regime, the nonuniform deformation features a e not observed although a variety of coarsened α morphologies are produced. Post-deformation heat treatment increases the amount of equiaxed α. The definition of the low and high temperature regimes along with the approximate influence of total strain allows the design of forging precesses in order to predict the distribution of final microstructure and properties in a finished part.

The new heat treatment, double solution treatments in the α+β region below the β transus and then ageing, is now being applied to a β -rich Ti-6Al-2Sn-4Zr-6Mo alloy to improve fracture toughness and fatigue properties. The β rich alloys such as Ti-6246 or Ti-6Al-6V-2Sn alloy can be produced in a large variety of microstructures,because of a large, nearly 40% of the β phase compared to that of about 18% in Ti-6Al-4V alloy.

It is now known to be very effective to control the volume fraction of the primary equiaxed α and the morphology of an acicular α phase produced from the transformed β phase by ageing.

The first solution treatment in the double solution treatment is performed as the first stage at the temperature near the β transus in order to control the volume fraction of the primary α phase and also, by a subsequent quenching, to produce a hexagonal α' martensite or an orthorhombic α" martensite, which may serve as the nucleation sites for the α phase. Then by the secondary solution treatment, which is conducted at the temperature lower than that of the first solution treatment, the secondary α phase nucleates and grows from the favourable precursor of α' or α".

The typical micrographs of the specimen double-solutionized together with the one solutionized ordinarily are shown in Fig. 5 (a) and (b), respectively (16).

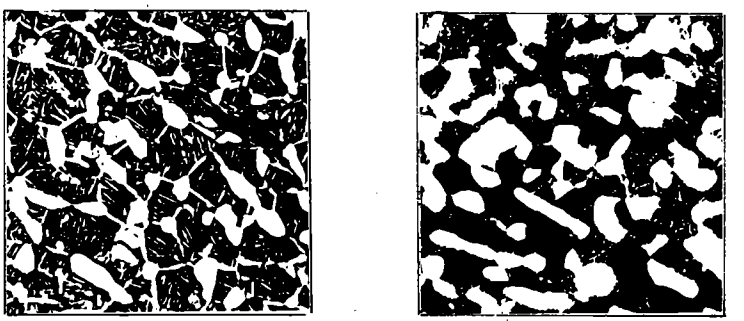

Fig. 5 : Comparison between the two solution treatments

(a) Optical micrograph of the specimen of Ti-6246 double-solutionized and aged; 940°Cx1hr AC + 830°Cx2hr AC + 573°Cx6hr AC

K_{Ic} : 103 kgf/mm$^{3/2}$,
$\sigma_{0.2}$: 115 kgf/mm^2, δ : 14%

(b) Optical micrograph of the specimen of Ti-6246 solutionized and aged; 910°Cx1hr AC + 573°Cx6hr AC

K_{Ic} : 78 kgf/mm$^{3/2}$,
$\sigma_{0.2}$: 119 kgf/mm^2, δ : 10%

Thus in the double-solution treatment, the first solution treatment decreases the amount of the primary α, and the secondary solution treatment results in producing coarse acicular α phase, which is effective for branching the cracks, and hence to improve the fracture toughness as shown the numerical values of K_{Ic} under Fig. 5.

Metastable β alloys

Metastable β alloys possess processing advantages over α + β phase alloys owing to a low flow stress at room temperature and elevated temperatures. Moreover, mechanical or physical properties can be controlled appropreately by processing and heat treatment conditions. Commercial applications of metastable β phase alloys, therefore, are extended over a wide range, particularly as high specific strength structural materials and ductile superconducting alloys.

It is recognized that two types of α phase, Type 1α (Burgers α) and Type 2α (non-Burgers α), and two transition phases, bcc β' phase and hexagonal ω phase appear during decomposition of β phase, strongly dependent on alloy composition, hot-working history and susequent heat treatment (1). Effect of these phases on mechanical properties is quite different each other. Therefore, it should be necessary to control microstructures precisely in order to obtain a β phase alloys with an excellent mechanical or physical properties.

Two transition phases could not been empolyed as strengthening precipitate, because the precipitation of β ' phase causes litte or no increase in strength (17), and the formation of ω phase usually results in severe reduction of fracture toughness (18 to 20). However, these phases are known to play an important role in nucleation of strengthening precipitates of fine-distributed α phase on the subsequent ageing. Both β' and ω phases distribute very finely and uni-

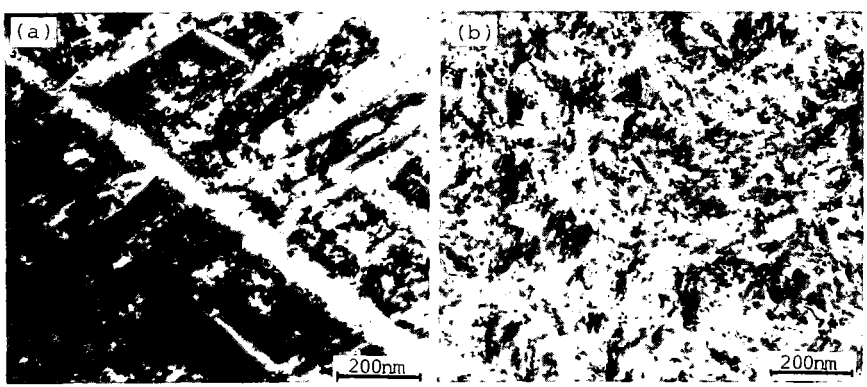

Fig. 6 : Transmission electron micrographs showing the effect of duplex ageing treatment in Ti-15Mo-5Zr-3Al alloy. (a) aged at 500°C for 500 min. directly after solutionized at 850°C. (b) duplex-aged at 300°C for 10⁴min. + at 500°C for 500 min.

formly, presenting a high density of α phase nuleation sites (17, 21). Therefore, the morphology and distribution of α phase may be controlled by the prior precipitation of β' or ω phase. Hence, desirable α phase dispersions can be attained efficiently by duplex ageing after solution treatment, i.c. an initial ageing at the relatively low temperature suitable for ω phase precipitation, and then the subsequent ageing at the higher temperature, where nucleation and growth of α phase takes place from ω phase (21 to 23).

For example, Fig. 6 are typical transmission electron micrographs showing the clear difference between two morphologies which results from the two kinds of ageing treatments. Fig. 6 (a) shows the well known Widmanstätten α phase plates, which is directly nucleated from the metastable β phase in Ti-15Mo-5Zr-3Al alloy aged at 500°C for 500 min. after quenching from 850°C. On the other hand, as shown in (b), the duplex ageing, initially at 300°C for 10 min. and then at 500°C for 500 min., leads to a very uniform dispersion of small, low aspect ratio α phase plates (24).

Terlinde et al. (25) have studied a variety of α - and ω - aged microstructures in the β-Ti alloy Ti-10V-2Fe-3Al. They were established by a combination of forging, solution treating and subsequent ageing and were characterized by different types of α -phase (primary α , secondary α , grain boundary α) as well as by the ω -phase. A detailed microscopical study revealed several deformation and fracture modes. It appears that at several sites stress and strain concentrations and subsequent void formation can occur and that the quantitative combinations of the different α -types determine which sites are active. The dominent deformation mode for the α + β solution treated and α -aged conditions was a strain localization in the aged matrix leading to voids at the interface between aged matrix and primary α -phase. In case of the β - solution treated and aged microstructures the grain boundary α leads to a strain localization in the soft α -film and to void nucleation at grain boundary triple points at lower macroscopic strains. Terlinde et al. have discussed in detail how varying size, volume fraction, and morphology of the α -phase affect the ductility. They have also found that the embrittling effect of ω -particles can be largely reduced by a grain refinement. The latter observation seems to confirm the mechanism on ω -embrittlement that fracture occurs by highly concentrated slip in a slip band and formation of very small microvoids (18, 26). Therefore, optimization of microstructures to improve the mechanical properties, particularly strength-ductility combination would be attained by controlling primary α , secondary α , grain boundary α and / or ω -phase.

The relation between two types of α -phases and mechanical properties is not still understood. One of the reasons may exist in the experimental difficulties in separating the individual effects of Type 1α and 2α morphology and volume fraction on the mechanical properties. Moreover, precipitation sequence seems to depend upon alloy systems and compositions. In beta Ti-14Mo-6Al (27), Ti-11.6Mo (27) and Ti-3Al-8V-6Cr-4Zr-4Mo (

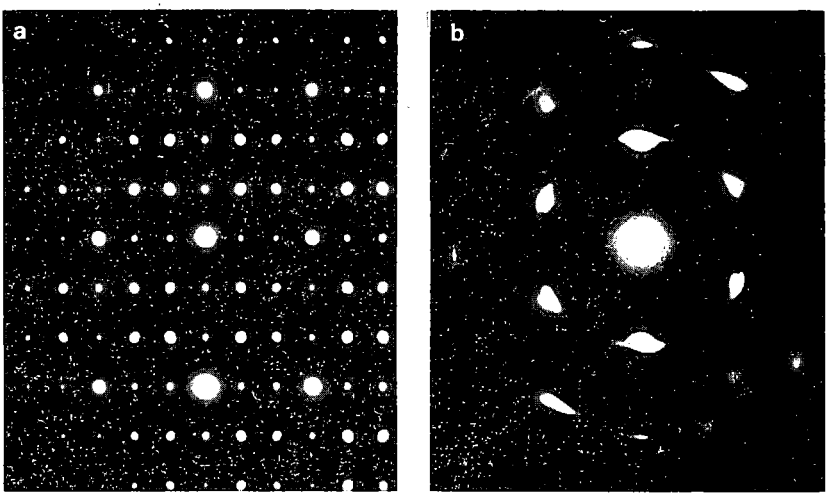

Fig. 7 : SAD patterns of Ti-15Mo-5Zr alloy. (a) solutionized at 400°C for 20 min. $\langle 111 \rangle_\beta$ zone with ω reflections. (b) solutionized and aged at 400°C for 100 min. $\langle 111 \rangle_\beta$ zone with Type 2 α reflections.

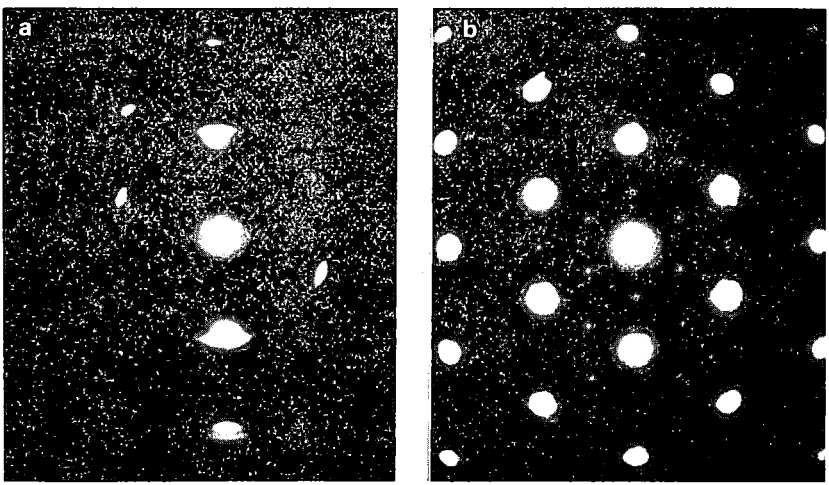

Fig. 8 : SAD patterns of Ti-20V alloy. (a) solutionized and aged at 400°C for 30 min. $\langle 111 \rangle_\beta$ zone with Type 2 α reflections. (b) solutionized and aged at 400°C for 3000 min. $\langle 111 \rangle_\beta$ zone with Type 1α reflections.

RMI38644) (17), the transition from Type 1 α to Type 2 α occurs during the prolong ageing, whereas in beta Ti-15Mo-5Zr (28), Ti-15Mo-5Zr-3Al (24) and Ti-10V-2Fe-3Al (29) the transition from ω to Type 2 α as well as the transition from Type 1α to Type 2α was observed. Hanada and Izumi have studied the crystallography and morphology of the precipitates formed during decomposition of metastable β phase of Ti-15Mo-5Zr alloys with or without 3 % Al mainly by a transmission electron microscopy (28). Fig. 7 shows SAD patterns of Ti-15Mo-5Zr alloy, where the typical ω and Type 2α reflections are clearly observed in (a) and (b), respectively. Further, the transition from Type 2α to Type 1α was reported to occur in Ti-20V by Takemura et al. (30), as shown in Fig. 8, where the above transition is verified. However, there exists a conflicting report that Type 2α was only a minor constituent during ageing of RMI38644 alloy (31). This discrepancies suggests that slight compositional variations could influence markedly on the formation of Type 2α.

The stress-induced martensitic transformation is reported to give a large elongation in β-solutionized Ti-10V-2Fe-3Al(29) while ductility in solutionized Ti-11.5-5.5-4.5 (32) and Ti-15-5 alloys (33) results mainly from mechanical twinning of {332} <113>, which is related to the stability of β-phase (34). With increasing stability of β-phase, the deformation mode changes from mechanical twinning to slip mechanism (35, 36).

One of the present authors (Murakami) would like to deal with electron energy loss spectroscopy (EELS) of ω phase in Ti-15-5-3 alloy, of which details are reported in this proceedings. Fig. 9 shows EELS spectra togehter with TEM images (37).

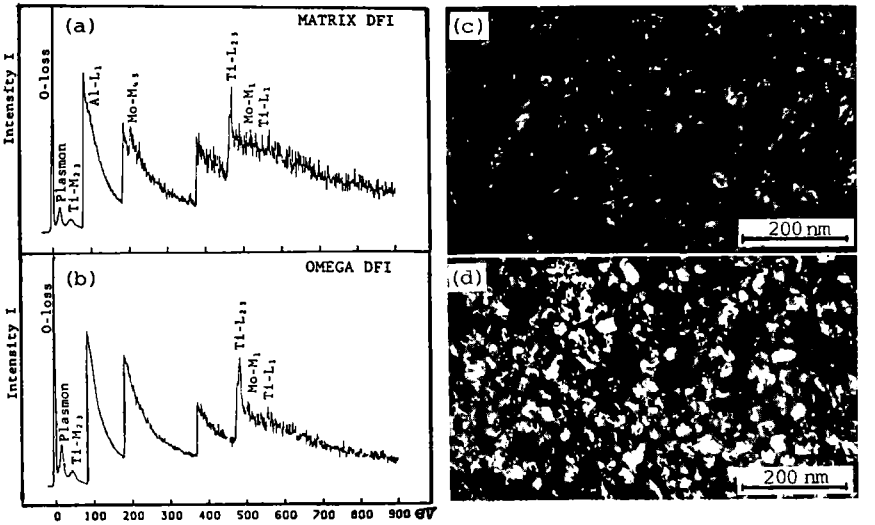

Fig. 9 : EELS spectra for matrix dark field image (a) and ω particles dark field image (b) for Ti-15-5-3 alloy aged 10 min. at 400°C, which correspond to matrix-DFI (c) and ω-DFI (d), respectively.

Beta Ti-Nb alloys for superconducting materials

The ß Ti-Nb alloys are presently used in commercial superconducting materials because of the easiness of fabrication and resistance against the stress produced when the magnetic field is generated. The characteristics of type II superconductors depend upon the crystal imperfections such as precipitates and dislocation sub-structures. Accordingly a metallographic investigation is necessary to obtain a quantitative knowledge of the spacial distribution of precipitates and the morphology of the dislocation sub-structures.

Osamura et al. (38) have studied the precipitation behaviour in thin foil and wire specimens of Ti-36 at% Nb and a commercial quaternary alloy of Ti-27Nb-5Zr-5Ta (in at%) mainly by means of small-angle X-ray scattering measurement and transmission electron microscopy.

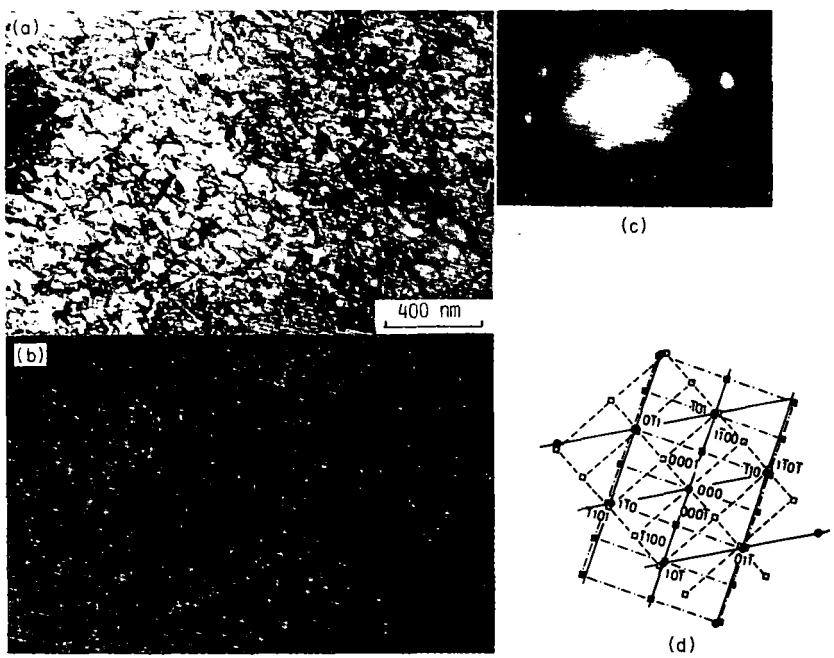

Fig. 10: Transmission electron micrographs of a Ti-36 at% Nb alloy aged for 1,000 min. at 380°C after 50% cold rolling. (a) Bright-field image, $[111]_\beta$ zone normal. (b) Dark-field image taken using $(1100)_\alpha$ spot. (c) SAD pattern (d) Key diagram, ● the β phase, and □ and ■ show two variants of the α phase.

The small-angle diffuse scattering observation was carried out at the various stages of precipitation, and it was concluded that the precipitate phase in the later stage of ageing was discriminated to be α .

The transmission electron microscopic observation was performed in parallel with the SAXS measurements. Fig. 10 , for instance, shows transmission electron micrographs of Ti-36 at% Nb alloy aged at 380°C for 1,000 min. after 50 % cold-rolling. From an analysis of a selected-area diffraction pattern (c), the incident beam was identified to be perpendicular to the (111) plane of the βmatrix and the other spots were assigned to the α phase, as shown in the key diagram (d). In the bright field image (a) there exists a homogeneously distributed dislocation structure. Although it is difficult to identify any precipitate in the bright-field image, the dark-field one (b) indicates clearly very thin thread-like α precipitates, which distribute very homogeneously.

By means of X-ray small-angle scattering, the change of relative integrated intensity and Guinier radius was measured during ageing in Ti- 36 at% Nb alloy. The integrated intensity in cold-rolled specimen was larger than that without cold-rolling, but in contrast the Guinier radius became smaller. The cold working was found to accelerate the precipitation rate of the α phase. The relative interparticle distance remained constant after a short time ageing for all spesimens with various rates of cold working. The precipitation behaviour of the commercial quarternary alloy was identified to be very similar to that of the binary alloy.

The ageing time dependence of relative integrated intensity an Guinier radius was measured using wire specimens aged at 380°C in relation to the rate of cold drawing. The intensity for the specimen with the diameter of 40 μm, i.e. the heavy drawn one have shown clearly to become large during a short ageing time compared with two specimens with the larger diameters of 60 and 110 μm, respectively, and the Guinier radius of 40 μm specimen increased more rapidly than the thicker ones.

Osamura and Ochiai (39) have found recently that α precipitates affect a more effective pinning force than dislocation substructures. In addition, Hanada et al. have confirmed that ω -phase forms during ageing of superconducting Ti-Nb alloys dependent upon compositions and ageing conditions (40).

Details of α or ω precipitation are not understood sufficiently, because precipitates accompanied with subband boundaries are too fine to study in detail and the phase relationships in Ti-Nb base alloy systems have not been established precisely (41). Nevertheless, to improve J_c in the high magnetic field cyclical processing of cold working and heat treatments and an alloying design for Ti-Nb base multicomponent systems are now under development. As the precipitation behaviour seems to be highly complicated, further systematic studies on heat treatments together with the effet of cold-working will be required to develop more excellent superconducting materials.

Intermetallic compounds

The intermetallic compounds of α_2-$TiAl_3$ and γ-TiAl have been of great interest for materials of construction for aircraft turbine engine. These ordered compounds are lighter and stiffer than conventional titanium alloys, and retain very high static strength, stiffness, and oxidation resistance at the higher temperatures than those attainable by conventional Ti alloys, though they show only very limited ductility below 600 °C. The goal of the compounds is to learn to improve the room temperature brittleness without saclificing the elevated temperature properties. The modes of deformation under the various testing conditions were studied in connection with microstructures, of which information are demanded.

A binary Ti-Al phase diagram as shown in Fig. 11, which is a little different from the reference (42), was presented by Martin et al. (43) based on the microstructural observation of the specimens quenched from a beta phase field in Ti_3Al and Ti_3Al + X (X: Nb and W) alloys. According their results, Ti_3Al

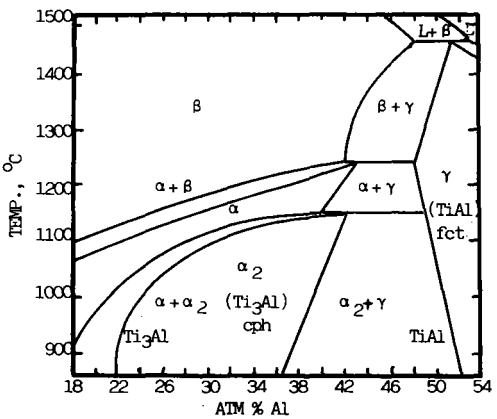

Fig. 11: Binary Ti-Al phase diagram
(by courtesy of Martin et al.)

binary and ternary alloys change to α_2 structure by quenching from the beta phase field at 1200°C into a boiling water. The transformation rate so rapid that no beta phase remains. The alloys transform martensitically. The additions of Nb and/or W decrease M_S temperature and result in a α_2 field structure. By reheating the quenched ternary alloys with α_2 structure to 900°C, beta phase particles stabilized by Nb and W precipitate heterogeneously.

The ordering kinetics is very rapid and the individual martensite plate in the quenched alloys contain small ordered domains. The Nb and W additions seem to retard the ordering rates. The fine α_2 structure improves either strength or ductility at room temperature. The ternary alloys tend to suffer

with phase unstability at high temperatures. Recrystallisation can occur along the prior beta grain boundaries in the ternary alloys during tensile deformation of 500 to 600°C after quenched into a boiling water from 1200°C and then aged for 8 hours at 900°C.

The other intermetallic compound, TiAl (gamma phase) with $L1_0$ has a promising characteristic of an excellent high temperture strength, creep resistance and low density. Recently it was shown that TiAl single crystals have a positive temperature dependence of yield stress as shown in Fig. 12 (44) , but it is not clear in polycrystals (45). TiAl-W alloy has a finer grain size than the stoichiometric gamma alloy,although both alloys are prepared by a powder metallurgical techniques and then extruded at 1400°C. The reason will be that the addition of W to TiAl alloy stabilizes the beta phase and then increases its volume fraction at high temperatures. This beta phase can persist in exsisting to a lower temperature than in the stoichiometric gamma alloy. Then further lowering the temperature, the beta phase decomposes into a lamellar structure of gamma and α_2 phases. Therefore, the microstructure of the ternary gamma alloy consists of equiaxied gamma grains surrounded by the lamellae of gamma and α_2 phases. The orientation relationship of the lamellae is $\{111\}_\gamma // \{0001\}_{\alpha_2}$ and $\langle 110\rangle_\gamma // \langle 11\bar{2}0\rangle_{\alpha_2}$ and the neighbouring γ lamellae are twin-related across $\{111\}$

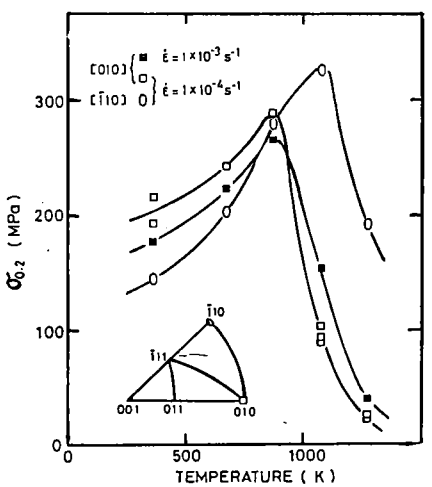

Fig. 12 : Temperature and strain rate dependences of 0.2% proof stress in TiAl single crystals with [010] and [$\bar{1}$10] orientations

planes. By ageing at 950°C small W rich precipitates nucleate heterogeneously on the internal boundaries. The fine structure of the alloy improves the creep resistance and the tensile strength without further loss inductility.

For further improvement of ductility, Tsujimoto et al.(46) Have intended to design an intermetallic compound TiAl base alloyas a dural structure of the TiAl and any metal phases.

For this purpose, metals which are able to be equilibriated with TiAl compound have been explored, resulting in the fact that Ag is only one metallic element which satisfies the requirement in this experimental scope from a preliminary study.

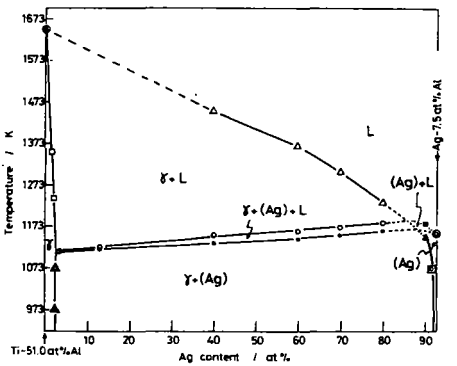

Fig. 13 : The vertical section through the composition of Ti-51.0 at% Al and Ag-7.5 at% Al line. (by courtecy of Tsujimoto et al.)

study. A constitutional diagram of a ternary Ti-Al-Ag system has been examined by means of electron probe microanalysis, X-ray diffractometry, scanning electron microscopy and differential thermal analysis. An isothermal section at 800°C and a vertical section through Ti-51 at% Al and Ag-7.5 at% Al line were determined. Fig. 13 shows the vertical section, where the TiAl compound constructs a pseudo-binary system with the (Ag) phase. The reaction temperature of TiAl + (Ag) + L ⟶ TiAl + (Ag) + L rises slightly with increasing Ag content, although it is located near the reaction temperature of TiAl + (Ag) + L ⟶ TiAl + L. The solubility of Ag in the TiAl phase decreases linearly at the temperature above 840°C, and then remains constant at the value of 2.4 at% Ag at the lower temperature than 800°C. The (Ag) phase contains about 8 at% Al and 0.6 at% Ti at the same temperature as above.

TiNi shape memory alloy

Recently, practical applications of shape memory effects have been developed in a wider field. An intermetallic compound TiNi is now known to be the most excellent shape memory alloy (47). This alloy can exhibit unique properties depending upon the compositions and heat treatments as well as processing. The high temperature phase in TiNi compound is considered to be CsCl (B2) (48), and the martensite to be a monoclinic distortion of the B19 structure (49). By complete

cycles, or additions of a small amount of Fe or Al, the intermediate phase with rhombohedral distortion appears clearly between B2 Parent phase and monoclinic martensite phase. In this temperature range, various authors have reported anomalous diffraction effects, which include scattering streaks (49 -50), extra diffraction spots at 1/3 and 1/2 positions of the B2 reciprocal lattice, the intensity of which increase on cooling (50). In addition in the temperature range the electrical resistivity increases remarkably on cooling from the high temperature B2 phase (48,49,52). The temperature at which electrical resistivity increases is generally defined as " M_S' ". According to a recent neutron diffraction and TEM study (53), the increase in electrical resistivity is thought to be caused by a transition to a pseudo-cubic incommensurate phase and then to a rhombohedral commensurate phase from the CsCl (B2) parent phase. The complex transformation proceeding to the martensite transformation is also concluded to originate in the exsistence of CDW. The anomalous increase effect can be enhanced by factors, which decrease M_S temperature, such as a appropriate selection of the final annealing temperature, thermal cycling in the transformation range, excess Ni concentration above the stoicheometric composition (54), or addition of other elements. These effects have now been called the " Premartensitic " phenomenon. The roll of premartensitic phase is now recognized to be very important for shape memory effect, especially in the two way memory, which is very useful for the practical application.

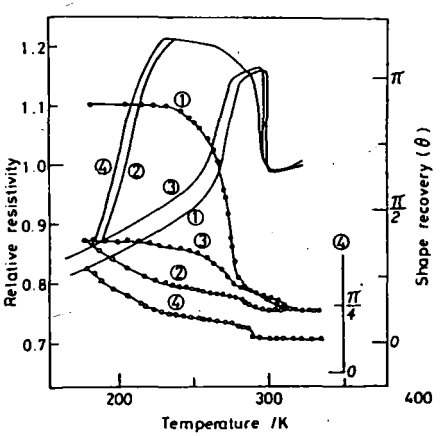

Fig. 14 : Electrical resistivity curve and corresponding the shape change behavior of Ti 50-Ni47-Fe2.5 alloy (by courtesy of Honma et al.)

Matsumoto and Honma have found that, when some parts of Ni atoms in TiNi are substituted by Fe atoms, M_S and M_S' are clear-

ly separated (55), and therefore it is very stable to employ Ti50- Ni50-x - Fe x for the syntherized investigation of the phase transformation in a TiNi alloy, particularly the parent to intermediate phase transformation. Fig. 14 shows electrical resistivity vs temperature curve and corresponding the shape change behavior for a Ti50-Ni47.5-Fe2.5 alloy. The electrical resistivity does not change during straightning specimen. It means that the specimen have been transformed to martensite. Recovery angle decreases rapidly near A_s and begins gradually to reach a constant value above A_s' during heating. During cooling, clear two-step shape change occurs. From there results, the parent to intermediate phase transformation contributes to shape change, especially in reversible shape memory effect, which are consistent with the investigation by Ling and Kaplow (56).

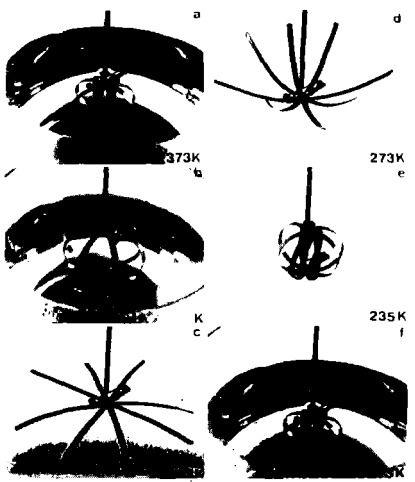

Fig. 15 : Spontaneous shape changes illustrating " all-round " shape memory effect. (by courtesy of Honma et al.)

It is also well known that in a Ni-rich TiNi alloy two-step transformation occurs by precipitated second phase particles. Several generating methods of reversible shape memory effect have the common principles in introducing internal stress field into a parent phase. Therefore, the above precipitation seems very likely to make an internal stress field. Recently Honma et al. (57) have developed a new type alloy, so-called " all-round memory alloy ", by utilizing the two-step transformation above mentioned. The alloy can display the shape memory effect either at high temperature or at low one, and also a complete reversals of shape by repeated heating and cooling. One of these alloys has a composition of Ti - Ni 51 at%, and was aged at 400 to 500 ^{o}C for 60 min. under

constrained condition after cold-rolled and annealed at 800 °C for 2 hours to remove strain. The shape change, as shown in Fig. 15 , from (a) the aged state at 100°C through (c) the cold-rolled and annealed state at room temperature and to (e) the exactly inverse state at -38°C. The spontaneous shape changes between (a) and (b), and state (c) and (e) are due to an intermediate phase transformation and martensitic transformation, respectively. Many small precipitates appear during the constrained ageing, and stress and strain between matrix and the precipitates result in the above shape memory. A Ti50-Ni47.5-Fe2.5 alloy can display a similar intermediate transformation, but precipitation does not occur (55). The shape memory of this alloy is confirmed to be reversible.

Acknowledgements

The authors gratefully acknowledge Drs. K.Kamei, S. Fujishiro, J.C. Williams, T. Tsujimoto, and T. Honma for permitting us to cite their published figures.

References

(1) Y.Murakami: " Titanium'80 Scence and Technology",AIME(1980) 153.
(2) G.Welsch, G.Lutiering, K.G.Gazioglu and W.Bunk: Met.Trans.,8A(1977) 169
(3) A.S.Ivanov and V.S.Tominsky: Phy.Met.Metall., 36(1973) 102.
(4) J.C.Williams, B.S.Hickman and D.H.Leslie: Met.Trans.,2(1971) 477.
(5) H.Margolin and P.Farrar: Ocean Eng., 1(1969) 327.
(6) H.Hamajima, G.Lutjering and S.Weissman: Met.Trans.,4(1973) 847.
(7) J.C.Williams and M.J.Blackburn: Trans. ASM, 60(1967) 373.
(8) H.Sasano, S.Komori and K.Kimur: J.Japan Inst. Met., 38(1974) 199.
(9) Yito and Y.Moriguchi : Collected Abst. Spring Meeting JIM,(1983) 287.
(10) T.Sigimoto, K.Kamei, S.Komatsu and K.Sugimoto: privat communication, (will appear in this proceedings)
(11) Y.Ito et al.: " Titanium'80 Science and Technology", AIME (1980)593.
(12) C.G.Rhodes and N.E.Paton: Met. Trans., 10A (1979) 209.
(13) H.Margolin,E.Levine,and M.Young: Met.Trans.,8A (1977) 373.
(14) Y.Mahajan,S.Nadiv and S.Fujishiro: Scripta Met., 16 (1982) 375.
(15) S.L.Semiatin, J.F.Thomas,Jr. and P.Daras: Met.trans. 14A (1983)2363.
(16) Y.Ito,T.Takashima and T.Nishimura: Collected Abst. Spring Meeting JIM, (1984) 161.
(17) C.G.Rhodes and N.E.Paton: Met.Trans., 8A (1977) 1749.
(18) J.C.Williams, B.s.Hickman and H.L.Marcus: Met. Trans., 2 (1971)1913.
(19) J.A.Feeney and M.J.Blackburn: Met. Trans., 1 (1970) 3309.
(20) S.Hanada and O.Izumi: Trans. Japan Inst. Met., 23 (1982) 85.
(21) F.H.Froes, C.F.Yolton, J.M.Capenos, M.G.H.Wells and J.C.Williams: Met.Trans., 11A (1980) 21.
(22) T.Nishimura, M.Nishigaki and S.Ohtani: J. Japan Inst. Met., 40 (1976) 219.
(23) G.M.Pennock, H.M.Flower and D.R.F.West:" Titanium"80 Science and Technology", AIME (1980) 1343.
(24) Y.Murakami, K.Nakao, Y.Yasuda, N.Tokushige, H.Yoshida and Y.Moriguchi: (will appear in this proceedings)
(25) G.T.Terlinde, T.W.Duerig and J . C. Williams: Met.Trans., 14A(1983) 2102.
(26) A.W.Bowen: " Titanium"80 Science and Technology", AIME (1980) 1317.

(27) C.G.Rhodes and J.C.Williams: Met. Trans., 6A (1975) 2103.
(28) S.Hanada and O.Izumi: Trans. Japan Inst. Met., 21 (1980) 210.
(29) T.W.Duerig, G.T.Terlinde and J.C.Williams: Met. Trans., 11A (1980) 1987.
(30) A.Takemura, S.Hanada and O.Izumi: Collected Abst. Autumn Meeting Japan Inst. Met., (1981) 378.
(31) T.J.Headley and H.J.Pack: Met. Trans., 10A (1979) 909.
(32) J.A.Roberson, S.Fujishiro, V.S.Arunachalam and C.M.Sargent: Met. Trans., 5 (1974) 2317.
(33) S.Hanada and O.Izumi: Met. Trans., 11A (1980) 1447.
(34) M.Oka and Y.Taniguchi: J. Japan Inst. Met., 42 (1978) 814.
(35) S.Hanada, A.Takemura and O.Izumi: Trans. Japan Inst. Met., 23 (1982) 507.
(36) M.Ozeki, S.Hanada and O.Izumi: Collected Abst. Autumn Meeting Japan Inst. Met., (1982) 415.
(37) Y.Murakami, K.Nakao, Y.Yasuda, N.Tokushige, H.Yoshida and Y.Moriguchi: (to appear in this proceedings)
(38) K.Osamura, E.Matsubara, T.Miyatani and Y.Murakami: Phil. Mag., 42 (1980) 575.
(39) K.Osamura and S.Ochiai: Collected Abst. Autumn Meeting Japan Inst. Met., (1983) 240.
(40) S.Hanada, A.Nagata, S.Den and O.Izumi: (to appear in J. Mat. Sci., (1984))
(41) D.C.Larbalestier: Superconductor Materials Science, ed. by S.Foner and B.B.Schwartz, Plenum Press,(1981) 133.
(42) E.Ence and H. Margolin: Trans AIME, 221, (1961) 151.
(43) P .L.Martin, H.A.Lipsitt, N.T.Nuhfer and J.C.Williams: " Titanium '80, Science and Technology, AIME (1980) 1245.
(44) T.Kawabata, Y.Takesono, T.Kanai and O.Izumi: (to appear in this proceedings)
(45) H.A.Lipsitt,D.Shechtman and R.E.Schafrik: Met. Trans., 6A (1975) 1991.
(46) K.Hashimoto, H.Doi and T. Tsujimoto: J.Japan Inst. Met., 47 (1983) 1036.
(47) C.M.Wayman and K.Shimizu: Met.Sci.J., 6 (1972) 175.
(48) D.P.Dautvich and G.R.Purdy: Can. Metall. Quart., 4 (1965) 129.
(49) G.D.Sandrock, A.J.Perkins and R.F.Heheman: Met. Trans., 2 (1971) 2769.
(50) K.Chanda and G.R.Purdy: J. App. Phys., 39 (1968) 2176.
(51) F.E.Wang, W.J.Bueler and S.J.Pikart: J.App.Phys., 36 (1965) 3232.
(52) C.M.Wayman, ICornelis and K.Shimizu: Scripta Met., 6 (1972) 115.
(53) C.M.Hwang, M.Meichle, M.B.Salamon and C.M.Wayman: Phil.Mag., 47 (1983) 9, 31, 177.
(54) T.Honma and H.Takei: J.Japan Inst.Met., 39 (1975) 175.
(55) M.Nishida and T.Honma: J.de phys., Coll. C4, suppl. au no. 12, Tom. 43. dèc. 1982, 225.
(56) H.C.Ling and R.Kaplow: Met.Trans., 11A (1980) 77.
(57) M.Nishida and T.Honma: Bull. Res. Inst. Mineral, Dressing and Metallurgy, Tohoku Univ., 38 (1982) 75.